Hindawi
International Journal of Antennas and Propagation
Volume 2018, Article ID 2094637, 6 pages
https://doi.org/10.1155/2018/2094637

Research Article

Detecting Load Resistance and Mutual Inductance in Series-Parallel Compensated Wireless Power Transfer System Based on Input-Side Measurement

Longzhao Sun, [1,2] Mingui Sun, [2] Dianguang Ma, [1] and Houjun Tang [1]

[1] *Department of Electrical Engineering, Shanghai Jiao Tong University, Shanghai 200240, China*
[2] *Department of Electrical and Computer Engineering, University of Pittsburgh, Pittsburgh, PA 15213, USA*

Correspondence should be addressed to Longzhao Sun; sunlongzhao@sjtu.edu.cn

Received 12 October 2017; Revised 21 February 2018; Accepted 4 March 2018; Published 25 June 2018

Academic Editor: Gino Sorbello

In wireless power transfer (WPT) system, the variations in load resistance and mutual inductance influence the output voltage and output current, making the system deviate from its desirable operating condition; hence, it is essential to monitor load resistance and mutual inductance. Using input-side measurement to detect load resistance and mutual inductance has great advantages, because it does not need any direct measurements on the receiving side. Therefore, it can remove sensors on the receiving side and eliminate communication system feeding back the load measurements. This paper investigates load resistance and mutual inductance detection method in series-parallel compensated WPT system. By measuring input current and input voltage, the equation for calculating load resistance is deduced; when the operating frequency is lower than or equal to the receiving-side resonant frequency, the rigorous mathematical derivations prove that load resistance can be uniquely determined by using only one measurement of input current and input voltage. Furthermore, the analytical expressions for identifying load resistance and mutual inductance are deduced. Experiments are conducted to verify the proposed method.

1. Introduction

Through magnetic coupling between transmitting and receiving coils, wireless power transfer (WPT) technique can deliver electrical energy from a source to a load without any electric wire [1, 2]. To improve system efficiency, compensation is needed to nullify inductive reactance. If input is voltage source, series compensation is required on transmitting side, and the receiving-side capacitor can be connected in parallel or series with the receiving coil. Therefore, voltage-fed WPT system can be categorized into series-parallel and series-series types [3].

Recently, WPT has been extensively applied in household appliances, robotics, portable electronic products, underwater equipment, implantable medical devices, and electric vehicle charging [4–8] because of its convenience, flexibility, reliability, and safety.

One challenge in WPT applications is the dynamic characteristics caused by load and mutual inductance variations. Different devices can be charged by WPT system, and the load values of these devices are different. Even for charging the same device, its battery equivalent resistance changes drastically as the charging process goes from constant current mode to constant voltage mode [9]. To provide more convenience for users, a receiver can be located with spatial freedom, which means the relative location of transmitter and receiver changes, thus resulting in mutual inductance variations. In dynamic WPT system (or roadway-powered electric vehicle), a vehicle that is running on a road can be wirelessly powered; in this case, the mutual inductance is time varying. These inevitable variations in load and mutual inductance will cause fluctuation in output voltage and output current, thus making WPT system deviate from its desirable operating condition. Therefore, monitoring load resistance and mutual inductance is essential for controlling and optimizing WPT system.

Generally, current and voltage sensors are installed on both transmitting and receiving sides, and a communication module is utilized to implement a feedback control between the transmitting and receiving sides. However, recent studies [10–16] show that load resistance and/or mutual inductance in series-series compensated WPT system can be estimated by measuring the input current and input voltage, eliminating sensors on receiving side and communication module; therefore it can significantly simplify circuit, reduce cost, and improve reliability. Paper [10] deduced the differential equation of the transmitting-side current; by investigating the variation rate of the approximate positive envelope of this current under different loading conditions, a load identification method was proposed. However, the effective detectable region was limited, and the accuracy in [10] got worse when the value of resistor was lower than 100 Ω. By root locus method, the whole detection region was categorized into two subregions; the mathematical equations of transient process in each subregion were established, and [11] presented a load identification model to increase the detection range. However, the load detection techniques in [10, 11] did not consider mutual inductance variations. By adding an extra capacitor into the transmitting side, WPT system could operate in two compensation modes via switching this capacitor; paper [12] combines the reflected impedance model and steady-state properties and presents a steady-state load detection method. The authors of [13] put forward a 1-port measurement approach, and the coupling factor and receiver quality factor could be monitored from the transmitter. However, these studies [10–16] did not investigate how to detect load resistance and mutual inductance in series-parallel compensated WPT system.

As discussed in [17, 18], series-parallel compensated topology plays an important role in WPT technology. Moreover, it is highlighted by the researchers [18] from Oak Ridge National Laboratory that they evaluated various compensation schemes and selected the series-parallel topology as the most appropriate one for voltage source operation.

This paper explores load resistance and mutual inductance detection in series-parallel compensated WPT system. The derivations in this paper are completely different from previous studies. Moreover, the proposed method is significantly intuitive and simple. To the best of our knowledge, this paper is the first work to prove that load resistance and mutual inductance in series-parallel compensated WPT system can be uniquely determined by using only one measurement of input current and input voltage. Furthermore, the analytical expressions for identifying load resistance and mutual inductance are deduced.

2. Modelling and Analysis

Figure 1 is the equivalent model of series-parallel compensated WPT system. V_S is the voltage source. The self-inductances of transmitting and receiving coils are L_1 and L_2, respectively; R_1 and R_2 denote the equivalent resistances of transmitting and receiving coils. Resonant capacitor C_1 is connected in series with transmitting coil, C_2 in parallel with receiving coil, forming series-parallel compensation topology. M is the mutual inductance between transmitting and receiving coils, and R_L is the load resistance.

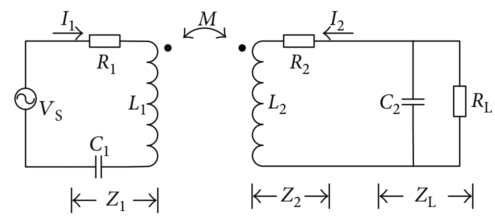

Figure 1: Equivalent circuit for series-parallel compensated WPT system.

Using Kirchhoff Voltage Law, the mathematical equations for series-parallel compensated WPT system in Figure 1 can be expressed as

$$\begin{aligned} V_S &= Z_1 \times I_1 + j\omega M \times I_2 \\ 0 &= j\omega M \times I_1 + (Z_2 + Z_L) \times I_2 \end{aligned}, \tag{1}$$

where $Z_L = R_L/(1 + j\omega C_2 R_L)$, $Z_1 = R_1 + j\omega L_1 + (1/j\omega C_1)$, $Z_2 = R_2 + j\omega L_2$.

Since the input current I_1 and input voltage V_S are measurable, the input impedance $Z_{in} = V_S/I_1$ is known. By calculating I_2 from (1) and substituting $Z_{in} = V_S/I_1$, the following equation can be obtained

$$Z_2 + Z_L = R_2 + j\omega L_2 + \frac{R_L}{1 + j\omega C_2 R_L} = \frac{\omega^2 M^2}{Z_{in} - Z_1}. \tag{2}$$

By separating the complex number equation (2) into the real part and imaginary part, (2) can be divided into two real number equations

$$\begin{aligned} R_2 + \frac{R_L}{1 + \omega^2 C_2^2 R_L^2} &= \omega^2 M^2 \operatorname{Re}\left(\frac{1}{Z_{in} - Z_1}\right), \\ \omega L_2 + \frac{-\omega C_2 R_L^2}{1 + \omega^2 C_2^2 R_L^2} &= \omega^2 M^2 \operatorname{Im}\left(\frac{1}{Z_{in} - Z_1}\right). \end{aligned} \tag{3}$$

To facilitate the derivation, a factor λ is introduced, and λ is defined as

$$\lambda = \frac{\operatorname{Re}(1/(Z_{in} - Z_1))}{\operatorname{Im}(1/(Z_{in} - Z_1))}. \tag{4}$$

By calculating M from (3) and substituting (4), (3) can be simplified as

$$\omega C_2 \left[\omega R_2 C_2 + \lambda\left(1 - \omega^2 L_2 C_2\right)\right] R_L^2 + R_L + R_2 - \lambda\omega L_2 = 0. \tag{5}$$

The coefficients of (5) are

$$a = \omega C_2 \left[\omega R_2 C_2 + \lambda\left(1 - \omega^2 L_2 C_2\right)\right], b = 1, c = R_2 - \lambda\omega L_2. \tag{6}$$

When the operating frequency ω is higher than the receiving-side resonant frequency ω_2 (i.e., $\omega_2 = 1/\sqrt{L_2 C_2}$), the numerical analysis indicates that there are two sets of positive roots in (5). For example, the same circuit parameters as listed in Section 4 are used, and the receiving-side resonant frequency is 209.6 kHz. When the WPT system operates at 215.0 kHz, if the input impedance Z_{in} is

$26.76\angle{-25.04^\circ}$, there are two sets of possible load resistance R_L and mutual inductance M combinations: $R_L = 311.3\,\Omega$ and $M = 8.7\,\mu$H, $R_L = 96.0\,\Omega$ and $M = 14.2\,\mu$H, which can lead to the identical input impedance Z_{in}.

The amplitude-frequency plot of input impedance Z_{in} in Figure 2(a) and phase-frequency plot in Figure 2(b) further clarify that two curves intersect at the same input impedance Z_{in} when operating at 215.0 kHz. This is the reason why load resistance R_L and mutual inductance M cannot be exactly identified based on one sample of input impedance Z_{in} when the operating frequency is higher than the receiving-side resonant frequency.

3. Load Resistance and Mutual Inductance Detection Method

Note that (5) has one positive root at least, corresponding to the actual value of the load resistance in series-parallel compensated WPT system. This paper aims to calculate theoretically and then validate experimentally the unique value of load resistance R_L (i.e., the solution of (5)).

When the operating frequency ω is lower than the receiving-side resonant frequency ω_2, that is, $\omega < 1/\sqrt{L_2C_2}$, it is found that there is only one positive root for load resistance R_L by solving (5), which means that load resistance R_L and mutual inductance M can be uniquely determined based on one measurement of input impedance Z_{in} only, and the rigorous derivations are as follows.

When $\omega < 1/\sqrt{L_2C_2}$, that is, $1 - \omega^2 L_2 C_2 > 0$, how to find the root of (5) is discussed under four cases:

Case 1. Assuming $a = \omega C_2[\omega R_2 C_2 + \lambda(1 - \omega^2 L_2 C_2)] = 0$, $\lambda = -\omega R_2 C_2/(1 - \omega^2 L_2 C_2) < 0$ and $c = R_2 - \lambda\omega L_2 > 0$ can be obtained. Solving (5), there is only one negative root; thus this case does not exist.

Case 2. Assuming $c = R_2 - \lambda\omega L_2 = 0$, $\lambda = R_2/\omega L_2 > 0$ and $a = \omega C_2[\omega R_2 C_2 + \lambda(1 - \omega^2 L_2 C_2)] > 0$ can be obtained. Solving (5), there are one zero root and one negative root for R_L; therefore this case is not existing.

Case 3. If $a = \omega C_2[\omega R_2 C_2 + \lambda(1 - \omega^2 L_2 C_2)] < 0$, $\lambda < -\omega R_2 C_2/(1 - \omega^2 L_2 C_2) < 0$ can be obtained, therefore $c = R_2 - \lambda\omega L_2 > 0$.

Case 4. If $c = R_2 - \lambda\omega L_2 < 0$, $\lambda > R_2/\omega L_2 > 0$ can be obtained, therefore $a = \omega C_2[\omega R_2 C_2 + \lambda(1 - \omega^2 L_2 C_2)] > 0$.

Based on the four cases discussed above, we conclude that a and c have opposite signs when $\omega < 1/\sqrt{L_2C_2}$. According to Vieta theorem, one and only one positive root exists by solving (5).

If $a > 0$, the detected load resistance is

$$R_L = \frac{-1 + \sqrt{1 - 4\omega C_2[\omega R_2 C_2 + \lambda(1 - \omega^2 L_2 C_2)](R_2 - \lambda\omega L_2)}}{2\omega C_2[\omega R_2 C_2 + \lambda(1 - \omega^2 L_2 C_2)]}. \tag{7a}$$

If $a < 0$,

$$R_L = \frac{-1 - \sqrt{1 - 4\omega C_2[\omega R_2 C_2 + \lambda(1 - \omega^2 L_2 C_2)](R_2 - \lambda\omega L_2)}}{2\omega C_2[\omega R_2 C_2 + \lambda(1 - \omega^2 L_2 C_2)]}. \tag{7b}$$

Substituting ((7a) and (7b)) into (3), the mutual inductance can be calculated by

$$M = \sqrt{\frac{R_2 + R_L + \omega^2 C_2^2 R_2 R_L{}^2}{\omega^2\left(1 + \omega^2 C_2^2 R_L^2\right)\mathrm{Re}(1/(Z_{in} - Z_1))}}. \tag{8}$$

When the operating frequency ω is equal to the receiving-side resonant frequency ω_2, we have $\omega = \omega_2 = 1/\sqrt{L_2C_2}$. According to (3) and (4), λ becomes

$$\lambda = \frac{R_2 + \omega^2 R_2 C_2^2 R_L^2 + R_L}{\omega L_2 + \omega^3 L_2 C_2^2 R_L^2 - \omega C_2 R_L^2}. \tag{9}$$

Substituting $\omega = \omega_2 = 1/\sqrt{L_2C_2}$, (9) can be simplified as

$$\lambda = \frac{R_2 + \omega^2 R_2 C_2^2 R_L^2 + R_L}{\omega L_2}. \tag{10}$$

Substituting $\omega = \omega_2 = 1/\sqrt{L_2C_2}$ and (10) into (5), the coefficients of (5) are

$$\begin{aligned} a &= \omega C_2\left[\omega R_2 C_2 + \lambda\left(1 - \omega^2 L_2 C_2\right)\right] = \omega^2 C_2^2 R_2 > 0, \quad b = 1, \\ c &= R_2 - \lambda\omega L_2 = -\left(\omega^2 R_2 C_2^2 R_L^2 + R_L\right) < 0. \end{aligned} \tag{11}$$

When $\omega = \omega_2 = 1/\sqrt{L_2C_2}$, the analysis shows that $a > 0$ and $c < 0$. According to Vieta theorem, one and only one positive root exists by solving (5). The detected value of load resistance is

$$R_L = \frac{-1 + \sqrt{1 - 4\omega^2 C_2^2 R_2 (R_2 - \lambda\omega L_2)}}{2\omega^2 C_2^2 R_2}. \tag{12}$$

Substituting (12) into (3), the mutual inductance can be calculated by

$$M = \sqrt{\frac{R_2 + R_L + \omega^2 C_2^2 R_2 R_L^2}{\omega^2\left(1 + \omega^2 C_2^2 R_L^2\right)\mathrm{Re}(1/(Z_{in} - Z_1))}} \tag{13}$$

The input current I_1 and input voltage V_S can be measured at an operating frequency ω, thus the input impedance $Z_{in} = V_S/I_1$ is known; the coil parameters (L_1, R_1, C_1, L_2, R_2, and C_2) are given. When the operating frequency is lower than the receiving-side resonant frequency, the detected values of load resistance R_L and mutual inductance M can be obtained by ((7a) and (7b)) and (8), respectively; when the operating frequency is equal to the receiving-side resonant frequency, the detected values of load resistance R_L and mutual inductance M can be obtained by (12) and (13), respectively.

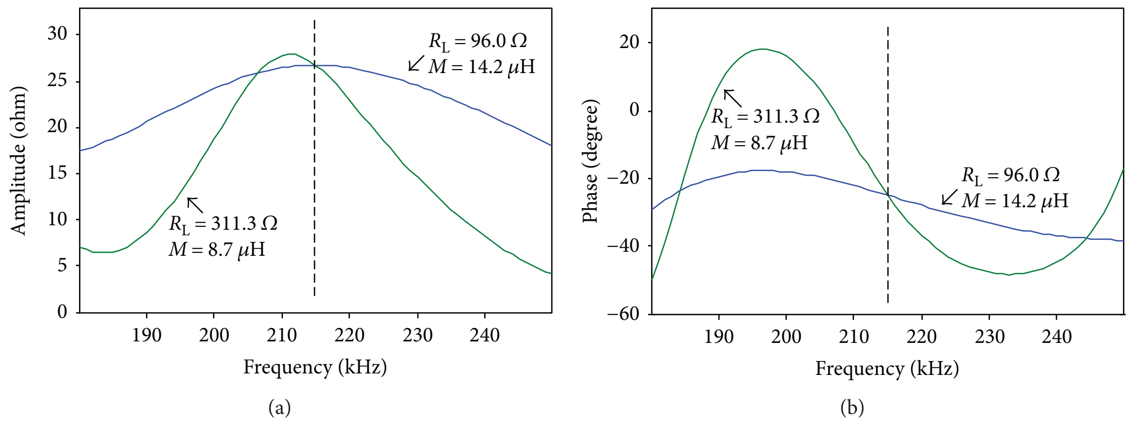

FIGURE 2: Input impedance spectral characteristics for two sets of load resistance R_L and mutual inductance M: (a) amplitude versus frequency; (b) phase versus frequency.

4. Experiment Analysis

To verify the proposed method for detecting load resistance and mutual inductance, a series-parallel compensated WPT prototype is implemented in this study, as shown in Figure 3. High-frequency input voltage drives the transmitting coil, and the transmitting coil is connected in series with the compensating capacitor. Through the inductive coupling between the transmitting coil and receiving coil, wireless power can be delivered to the receiving coil. The receiving coil is connected in parallel with the compensating capacitor, and the output voltage feeds the load. The parameters of transmitting coil are $L_1 = 27.3\,\mu$H, $R_1 = 0.425\,\Omega$, and $C_1 = 20.53$ nF. The parameters of receiving coil are $L_2 = 27.9\,\mu$H, $R_2 = 0.531\,\Omega$, and $C_2 = 20.67$ nF, and the receiving-side resonant frequency is 209.6 kHz.

When the WPT system operates at a specific frequency that is lower than or equal to the receiving-side resonant frequency, the input current I_1 and input voltage V_S are measured, and then the input impedance $Z_{in} = V_S/I_1$ can be obtained. These known information are utilized by the proposed detection method in Section 3 to obtain the load resistance and mutual inductance.

When a resistor of $55\,\Omega$ is utilized as the load, and the mutual inductance varies from 6.8 μH to 13.4 μH, the proposed method for detecting the load resistance and the mutual inductance is implemented, and the results are presented in Figure 4. In Figure 4(a), the dots and the diamonds denote the actual load resistance R_L and the detected load resistance $R_L{}^*$, respectively. Figure 4(b) shows how detected mutual inductance M^* varies with the actual mutual inductance M.

Using the same method, when mutual inductance is 10.7 μH and the load varies from $12\,\Omega$ to $82\,\Omega$, the experiments have been conducted to detect the mutual inductance and load resistance, and the results are shown in Figure 5. In Figure 5(a), the dots and the diamonds represent the actual mutual inductance M and the detected mutual inductance M^*, respectively. Figure 5(b) presents the plot of detected load resistance $R_L{}^*$ when actual load resistance R_L varies.

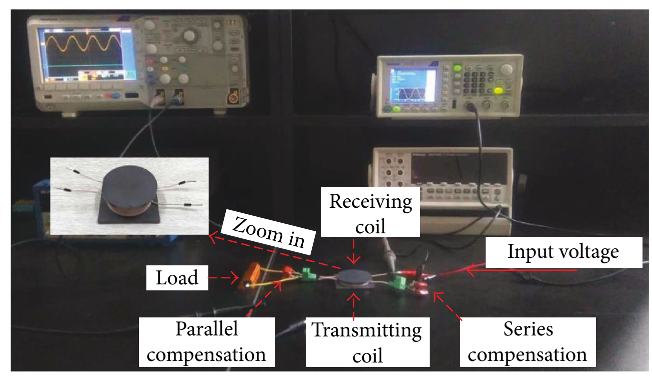

FIGURE 3: Photograph of the series-parallel compensated WPT experimental setup.

Based on the analysis of Figures 4 and 5, using the measured value of input current and input voltage, the load resistance and mutual inductance can be uniquely determined by the proposed method. Furthermore, it can be observed that the detected results of load resistance and mutual inductance agree well with their actual values, which validates the proposed detection method.

5. Conclusion

This paper thoroughly investigates load resistance and mutual inductance detection method in series-parallel compensated WPT system. The derivations and conclusions presented in this paper are brand new compared with previous studies. Moreover, the proposed method is significantly intuitive and simple.

When the operating frequency is lower than or equal to the receiving-side resonant frequency, the detailed mathematical derivations prove that the load resistance and mutual inductance can be uniquely determined based on one measurement of input current and input voltage only. And the analytical expressions for identifying load resistance and mutual inductance are deduced for the first time. Furthermore, a series-parallel compensated WPT

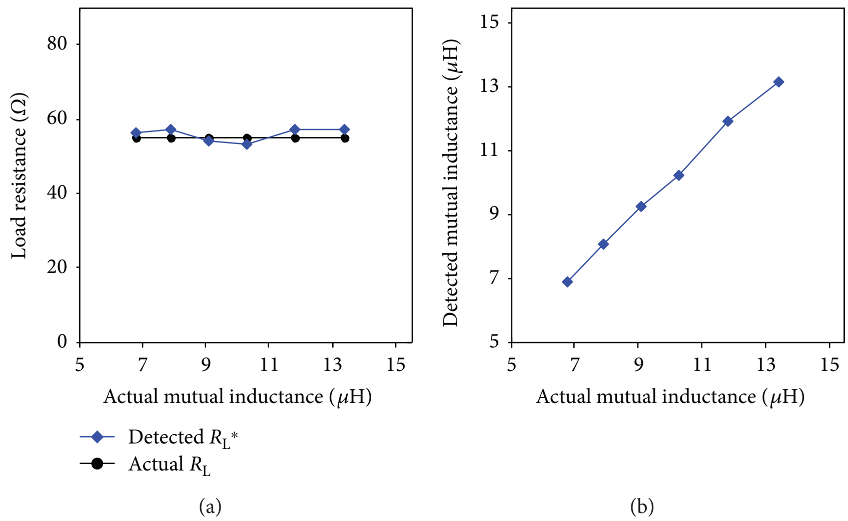

Figure 4: Detected results of (a) load resistance and (b) mutual inductance when actual mutual inductance varies.

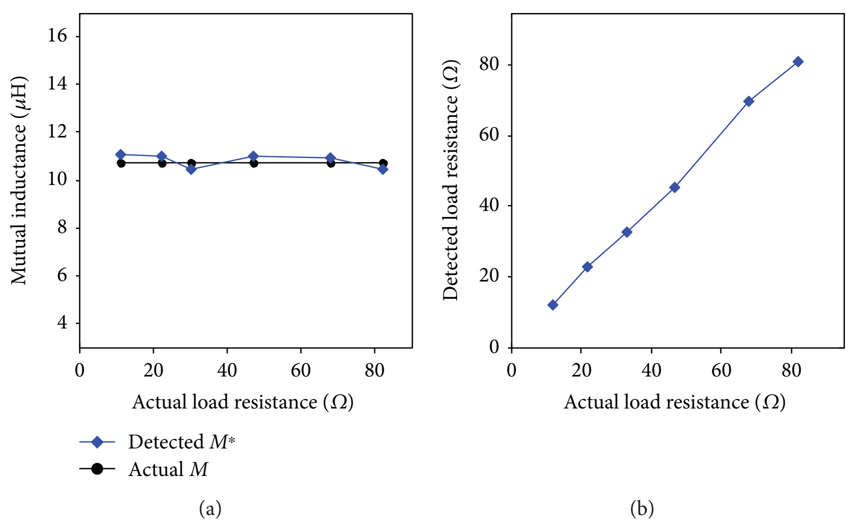

Figure 5: Detected results of (a) mutual inductance and (b) load resistance when actual load resistance varies.

prototype is built, and the experimental results confirm the proposed method.

This work can be applied to dynamically monitor the load status and the coupling relationship between the transmitting coil and receiving coil in series-parallel compensated WPT system; moreover, only one measurement of input current and input voltage is needed, thus making the proposed method straightforward.

Conflicts of Interest

The authors declare that there are no conflicts of interest.

Acknowledgments

This work was supported by China Scholarship Council and Chinese National Natural Science Foundation (U1604136).

References

[1] S. Assawaworrarit, X. Yu, and S. Fan, “Robust wireless power transfer using a nonlinear parity–time-symmetric circuit,” *Nature*, vol. 546, no. 7658, pp. 387–390, 2017.

[2] Y. Luo, Y. Yang, S. Chen, and X. Wen, “A frequency-tracking and impedance-matching combined system for robust wireless power transfer,” *International Journal of Antennas and Propagation*, vol. 2017, Article ID 5719835, 13 pages, 2017.

[3] M. E. Halpern and D. C. Ng, “Optimal tuning of inductive wireless power links: limits of performance,” *IEEE Transactions on Circuits and Systems I: Regular Papers*, vol. 62, no. 3, pp. 725–732, 2015.

[4] C. C. Mi, G. Buja, S. Y. Choi, and C. T. Rim, “Modern advances in wireless power transfer systems for roadway powered electric vehicles,” *IEEE Transactions on Industrial Electronics*, vol. 63, no. 10, pp. 6533–6545, 2016.

[5] G. Monti, L. Corchia, E. de Benedetto, and L. Tarricone, “A wearable wireless energy link for thin-film batteries charging,”

International Journal of Antennas and Propagation, vol. 2016, Article ID 9365756, 9 pages, 2016.

[6] T. Kan, R. Mai, P. P. Mercier, and C. Mi, "Design and analysis of a three-phase wireless charging system for lightweight autonomous underwater vehicles," *IEEE Transactions on Power Electronics*, vol. 33, p. 1, 2017.

[7] C. Xiao, D. Cheng, and K. Wei, "An LCC-C compensated wireless charging system for implantable cardiac pacemakers: theory, experiment, and safety evaluation," *IEEE Transactions on Power Electronics*, vol. 33, no. 6, pp. 4894–4905, 2017.

[8] D.-W. Seo, J.-H. Lee, and H. Lee, "Integration of resonant coil for wireless power transfer and implantable antenna for signal transfer," *International Journal of Antennas and Propagation*, vol. 2016, Article ID 7101207, 7 pages, 2016.

[9] X. Qu, H. Han, S.-C. Wong, C. K. Tse, and W. Chen, "Hybrid IPT topologies with constant current or constant voltage output for battery charging applications," *IEEE Transactions on Power Electronics*, vol. 30, no. 11, pp. 6329–6337, 2015.

[10] Z.-H. Wang, Y.-P. Li, Y. Sun, C.-S. Tang, and X. Lv, "Load detection model of voltage-fed inductive power transfer system," *IEEE Transactions on Power Electronics*, vol. 28, no. 11, pp. 5233–5243, 2013.

[11] S. Hu, Z. Liang, Y. Wang, J. Zhou, and X. He, "Principle and application of the contactless load detection based on the amplitude decay rate in a transient process," *IEEE Transactions on Power Electronics*, vol. 32, no. 11, pp. 8936–8944, 2017.

[12] Y.-G. Su, H.-Y. Zhang, Z.-H. Wang, A. P. Hu, L. Chen, and Y. Sun, "Steady-state load identification method of inductive power transfer system based on switching capacitors," *IEEE Transactions on Power Electronics*, vol. 30, no. 11, pp. 6349–6355, 2015.

[13] H. S. Jang, J. W. Yu, and W. S. Lee, "1-port measurement method of the coupling factor and receiver Q for spatial and state freedom in wireless power transfer systems," *IEEE Transactions on Antennas and Propagation*, vol. 64, no. 9, pp. 4098–4102, 2016.

[14] J. Yin, D. Lin, C. K. Lee, and S. Y. Hui, "Front-end monitoring of multiple loads in wireless power transfer systems without wireless communication systems," *IEEE Transactions on Power Electronics*, vol. 31, no. 3, pp. 2510–2517, 2016.

[15] J. Yin, *Monitoring system parameters and loads in wireless power transfer systems without radio-frequency communication system, [Ph.D. thesis]*, University of Hong Kong, Hong Kong, 2015.

[16] X. Dai, X. Li, Y. Li, and A. P. Hu, "Maximum efficiency tracking for wireless power transfer systems with dynamic coupling coefficient estimation," *IEEE Transactions on Power Electronics*, vol. 33, no. 6, pp. 5005–5015, 2017.

[17] J. Kim, J. Kim, S. Kong et al., "Coil design and shielding methods for a magnetic resonant wireless power transfer system," *Proceedings of the IEEE*, vol. 101, no. 6, pp. 1332–1342, 2013.

[18] J. M. Miller, O. C. Onar, and M. Chinthavali, "Primary-side power flow control of wireless power transfer for electric vehicle charging," *IEEE journal of Emerging and selected topics in power electronics*, vol. 3, no. 1, pp. 147–162, 2015.


Journal of Engineering
The Scientific World Journal
International Journal of Rotating Machinery
Journal of Sensors
Advances in Multimedia
Advances in Civil Engineering
Journal of Control Science and Engineering
Journal of Robotics
Hindawi
Submit your manuscripts at
www.hindawi.com
Journal of Electrical and Computer Engineering
Advances in OptoElectronics
VLSI Design
International Journal of Navigation and Observation
Modelling & Simulation in Engineering
International Journal of Aerospace Engineering
International Journal of Chemical Engineering
International Journal of Antennas and Propagation
Active and Passive Electronic Components
Shock and Vibration
Advances in Acoustics and Vibration